

## AN ANALYTICAL STUDY OF RECTANGULAR PLATES UNDER TRIANGULARLY DISTRIBUTED REGIONAL LOADS

三角形荷重が局部的に作用する二隣辺固定二辺自由版の弾性解析とその応用

Kazuo KANEDA\*, Shigeo IRAHA\*\*, Tetsuo TAKAMINE\*\*\*, Kei SHIMABUKU\*\*\*\*  
金田一男, 伊良波繁雄, 高嶺哲夫, 島袋 佳

\* Member MS Hope Design Co.,Ltd (〒902-0064 3-3-5 Yorimiya, Naha city, Okinawa)

\*\* Member PhD Prof. Dept. Eng. Univ. of the Ryukyus

(〒903-0213 1 Nisihara Aza Senbaru, Okinawa)

\*\*\* Hope Design Co.,Ltd (〒902-0064 3-3-5 Yorimiya, Naha city, Okinawa)

\*\*\*\* MS Hope Design Co.,Ltd (〒902-0064 3-3-5 Yorimiya, Naha city, Okinawa)

An analytical study and the application of the rectangular plates with two adjacent sides fixed and other two sides free under triangularly distributed regional loads are shown in this paper. The Type-3 Fourier series analytical method proposed by Higashi, Y. and Komori, K. was developed here. A comparison study for the bending moments of the fixed sides of the rectangular plates was carried out with Finite Element Method (FEM). The rationality and the applicability of analytical results were estimated and discussed. The figures of the coefficients of the bending moments and the shearing forces on the fixed sides of the rectangular plates were presented for the designer.

**Key Words:** *triangularly distributed regional load, Fourier series analysis, rectangular plate, finite element method, bending moment, shearing force*

### 1. Introduction

The rectangular plates with two adjacent sides fixed and the other sides free are commonly used in many civil engineering structures, such as, the wing walls of the bridge abutment, the corner retaining walls of a storage-reservoir and the corner slabs of the veranda of a building. The loads acting on the rectangular plates include the uniform, triangular and trapezoidal distributed loads. Sometimes, the triangularly distributed regional loads, such as, earth pressure or residual water pressure also act on the rectangular plates. Higashi, Y. and Komori, K.<sup>1)</sup> have investigated the uniformly loaded rectangular plates in the same conditions using the method of Fourier series analysis. The authors<sup>2)</sup> have developed this method for the cases of triangular and trapezoidal distributed loads acting on the rectangular plates.

In this way, the basic analytical method by using Fourier series for the rectangular plates has been solved. Since the design-data of the rectangular plate that fixed-supported by two adjacent sides and loaded by the triangularly distributed regional load have not been offered, it is greatly inconvenient for the designers. From this point of view, it is necessary to consider the analytical results of such kind of plates investigated herein.

This paper shows the analytical study and application of the regionally and triangularly loaded rectangular plates in the condition of two adjacent sides fixed and other two sides free. The Type-3 Fourier series analytical method proposed by Higashi, Y. and Komori, K. was developed for this investigation. A comparison study for the bending moments of the fixed sides of the rectangular plates was carried out with FEM. The rationality and the applicability of the analytical results were estimated and discussed. Also, the figures of the coefficients of the bending moments and the shearing forces on the fixed sides of the rectangular plates were presented for the designer.

### 2. Fourier Series Analysis

#### 2.1 Analytical Model and Fundamental Assumptions

The model employed in this study is shown in Fig. 1. The rectangular plate is supported by the fixed sides  $x=a$  and  $y=b$  respectively. The triangularly distributed regional load  $P(x, y)$  was considered as regional earth pressure or residual water pressure, and the load was distributed uniformly along the  $x$  axis and triangularly along the  $y$  axis in the range of  $b_0 < y < b$ . The maximum intensity of the triangularly distributed regional load

is described as  $P_{max}$ . It is assumed that the x and y axes are taken parallel to the sides of the rectangular plate.

In this study, the following assumptions are used for analysis:

- (1) The deflections are small in comparison with the thickness  $t$  of the rectangular plate.
- (2) The rectangular plate is an isotropic elastic thin plate with elasticity modulus  $E$  and Poisson's ratio  $\nu$ .
- (3) The "plane section assumption" is applicable, i.e., plane sections remain plane before and after bending.

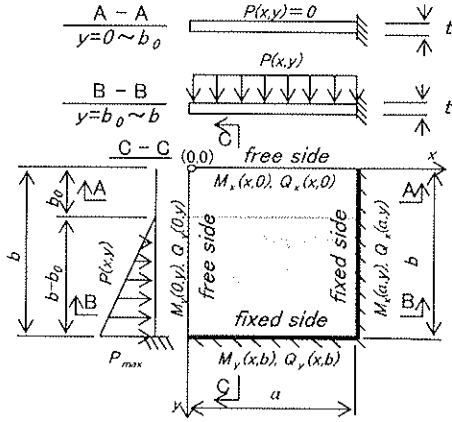


Fig. 1 Model for Fourier series analysis

## 2.2 Basic Equation for Deflection of a Plate

It is known that the basic equation for the deflection of a plate can be expressed as:

$$\frac{\partial^4 W(x, y)}{\partial x^4} + 2 \frac{\partial^4 W(x, y)}{\partial x^2 \partial y^2} + \frac{\partial^4 W(x, y)}{\partial y^4} = \frac{P(x, y)}{D} \quad (1)$$

where,  $P(x, y)$  is the optional lateral load acting on the plate,  $D$  is the flexural rigidity of the plate that can be represented in the following form:

$$D = \frac{Et^3}{12(1-\nu^2)} \quad (2)$$

$W(x, y)$  is the deflection of the plate at any point  $(x, y)$  and can be obtained from Eq. (3):

$$W(x, y) = W_1(x, y) + W_2(x, y) \quad (3)$$

where,  $W_1(x, y)$  represents the particular solution for the deflection of the rectangular plate which determined by the triangularly distributed regional load  $P(x, y)$ . Hence,  $W_1(x, y)$  is determined in such a form so as to satisfy the boundary conditions on the sides  $x=0$ ,  $a$ , and  $y=0$ ,  $b$ , respectively, and also to satisfy the Eq. (1) of the deflection surface. The expression of

$W_1(x, y)$  is shown in the next section.

Since, the sides  $x=a$  and  $y=b$  of the rectangular plate as shown in Fig. 1 are fixed, the tangent plane to the deflected middle surface along these edges coincides with the initial position of the middle plane of the plate. The boundary conditions are:

$$x = a, \quad \frac{\partial W}{\partial x}(a, y) = 0 \quad (4)$$

$$y = b, \quad \frac{\partial W}{\partial y}(x, b) = 0 \quad (5)$$

Also, the sides  $x=0$  and  $y=0$  of the rectangular plate are free and these edges can rotate freely with respect to the edge line respectively. That is to say, there are no bending moments  $M_x(0, y)$  and  $M_y(x, 0)$  along these edges. In this case, analytical expressions for the boundary conditions are:

$$x = 0,$$

$$M_x(0, y) = -D \left[ \frac{\partial^2 W}{\partial x^2}(0, y) + \nu \frac{\partial^2 W}{\partial y^2}(0, y) \right] = 0 \quad (6)$$

$$y = 0,$$

$$M_y(x, 0) = -D \left[ \frac{\partial^2 W}{\partial y^2}(x, 0) + \nu \frac{\partial^2 W}{\partial x^2}(x, 0) \right] = 0 \quad (7)$$

The expression  $W_2(x, y)$  as shown in the right side of Eq. (3) is the general solution of the rectangular plate and evidently has to satisfy the equation as follows:

$$\frac{\partial^4 W_2(x, y)}{\partial x^4} + 2 \frac{\partial^4 W_2(x, y)}{\partial x^2 \partial y^2} + \frac{\partial^4 W_2(x, y)}{\partial y^4} = 0 \quad (8)$$

$W_2(x, y)$  must be chosen in such a manner so as to make  $W(x, y)$  satisfying all boundary conditions of the rectangular plate as shown in Fig. 1. In this study, a form of Fourier series that suggested by Higashi, Y. and Komori, K<sup>1)</sup>, is used for the general solution, the expression is:

$$W_2(x, y) = \sum_{n=1}^{\infty} \left\{ F_{x1} \frac{M_{an}}{D\beta^2} + [F_{x2} - F_{x3}] \frac{\theta_{an}}{\beta} \right\} \frac{\cos \beta y}{2 \cosh \beta a} + \sum_{m=1}^{\infty} \left\{ F_{y1} \frac{M_{bm}}{D\alpha^2} + [F_{y2} - F_{y3}] \frac{\theta_{bm}}{\alpha} \right\} \frac{\cos \alpha x}{2 \cosh \alpha b} \quad (9)$$

where, the symbols  $F_{x1}$ ,  $F_{x2}$  and  $F_{x3}$  are the function of  $x$  only and expressed in the forms:

$$\left. \begin{aligned} F_{x1} &= \beta a \tanh \beta a \cosh \beta x - \beta x \sinh \beta x \\ F_{x2} &= [(1-\nu)\beta a \tanh \beta a - 1 - \nu] \sinh \beta(a-x) \\ F_{x3} &= (1-\nu)\beta(a-x) \cosh \beta(a-x) \end{aligned} \right\} \quad (10)$$

Similarly, the symbols  $F_{y1}$ ,  $F_{y2}$  and  $F_{y3}$  are the function of  $y$  only and expressed in the forms:

$$\left. \begin{aligned} F_{y1} &= \alpha b \tanh \alpha b \cosh \alpha y - \alpha y \sinh \alpha y \\ F_{y2} &= [(1-\nu)\alpha b \tanh \alpha b - 1 - \nu] \sinh \alpha(b-y) \\ F_{y3} &= (1-\nu)\alpha(b-y) \cosh \alpha(b-y) \end{aligned} \right\} \quad (11)$$

where, a and b are the lengths of the rectangular plate along the x and y directions respectively.  $M_{a_n}$ ,  $A_m$ ,  $M_{b_m}$  and  $B_m$  are the integration constants. and are the notations which can be written as follows:

$$\alpha = \frac{2m-1\pi}{2a}, \quad \beta = \frac{2n-1\pi}{2b} \quad (12)$$

and m and n are the integer numbers,  $m=1, 2, 3, \dots$ ,  $n=1, 2, 3, \dots$ .

It is clear that Eq. (9) can satisfy the boundary conditions, such as, the deflections on the sides  $x=a$  and  $y=b$ , and the shearing forces on the sides  $x=0$  and  $y=0$  are zero.

### 2.3 Particular Solution for the Deflection of the Rectangular Plate

As shown in Fig. 1, the triangularly distributed regional loads can be expressed by the following form:

$$P(x, y) = \left(\frac{y-b_0}{b-b_0}\right) P_{\max} \quad (b_0 \leq y \leq b) \quad (13)$$

where,  $b_0$  is the length at which the load equal to zero, and  $P_{\max}$  is the maximum value of the triangularly distributed regional loads. If, in particular,  $b_0=0$ , Eq. (13) yields  $P(x, y)=y/b \cdot P_{\max}$ , which is the expression for the triangularly loaded rectangular plates.

In this study, the particular solution  $W_1(x, y)$  as shown in Eq. (3) can be expressed in the form of a double trigonometric series of  $\cos x$  and  $\cos y$  from Eq. (13), and the expression can be expressed as follows:

$$W_1(x, y) = \frac{4P_{\max}}{abD} \sum_{m=1}^{\infty} \sum_{n=1}^{\infty} \frac{-(-1)^m}{\alpha(\alpha^2 + \beta^2)^2} \times \left[ \frac{-(-1)^n}{\beta} - \frac{1}{b\beta^2} \cdot \frac{\cos \beta b_0}{(1-b_0/b)} \right] \cos \alpha x \cdot \cos \beta y \quad (14)$$

In order to determine the integration constants  $M_{a_n}$ ,  $A_m$ ,  $M_{b_m}$  and  $B_m$ , the simultaneous equations that satisfy the boundary conditions as shown in Eqs. (4) to (7) will be developed in the next section. In order to do so, the Eq. (14) must be exchanged by the form of a single trigonometric series of  $\cos x$  or  $\cos y$ , and their expressions are given by Eqs. (15) and (16) respectively.

$$W_1(x, y) = \frac{2P_{\max}}{bD} \sum_{n=1}^{\infty} \frac{-(-1)^n}{\beta^3} \left[ 1 - \frac{(\beta \alpha \tanh \beta \alpha + 2) \cosh \beta x - \beta x \sinh \beta x}{2 \cosh \beta a} \right] \times \left[ 1 + \frac{(-1)^n}{b\beta} \cdot \frac{\cos \beta b_0}{(1-b_0/b)} \right] \cos \beta y \quad (15)$$

$$W_1(x, y) = \frac{2P_{\max}}{aD} \sum_{m=1}^{\infty} \frac{-(-1)^m}{\alpha^3} \times \left\{ 1 - F_{y4} - \left( 1 - \frac{y}{b} - F_{y5} \right) \frac{\cos \beta b_0}{(1-b_0/b)} \right\} \times \cos \alpha x \quad (16)$$

where, the symbols  $F_{y4}$  and  $F_{y5}$  are expressed in the following forms:

$$\left. \begin{aligned} F_{y4} &= \frac{(\alpha b \tanh \alpha b + 2) \cosh \alpha y - \alpha y \sinh \alpha y}{2 \cosh \alpha b} \\ F_{y5} &= \frac{(\alpha b \tanh \alpha b + 3) \sinh \alpha(b-y) - \alpha(b-y) \cosh \alpha(b-y)}{2 \alpha b \cosh \alpha b} \end{aligned} \right\} \quad (17)$$

### 2.4 Inducement of Simultaneous Equations

The integration constants  $M_{a_n}$ ,  $A_m$ ,  $M_{b_m}$  and  $B_m$  as shown in Eq. (9) must be determined by satisfying the boundary conditions from Eqs. (4) to (7). For convenience, these integration constants can be exchanged by using the notations:

$$\left. \begin{aligned} \psi_{a_n} &= \frac{M_{a_n}}{P_{\max} \cdot a^2}, \quad \varphi_{A_n} = \frac{D \cdot \theta_{A_n}}{P_{\max} \cdot a^3} \\ \psi_{b_m} &= \frac{M_{b_m}}{P_{\max} \cdot a^2}, \quad \varphi_{B_m} = \frac{D \cdot \theta_{B_m}}{P_{\max} \cdot a^3} \end{aligned} \right\} \quad (18)$$

Substituting the equations (9) and (15) into the boundary condition Eq. (4), when  $n = 1, 2, 3, \dots$ , the equation that includes the notations  $\psi_{a_n}, \varphi_{A_n}, \psi_{b_m}, \varphi_{B_m}$  can be obtained as follows:

$$\begin{aligned} & \frac{\beta \alpha + \sinh \beta \alpha \cosh \beta \alpha}{2 \cosh^2 \beta a} \frac{\psi_{a_n}}{\beta \alpha} \\ & + \frac{(1-\nu)\beta \alpha \sinh \beta \alpha - 2 \cosh \beta \alpha}{2 \cosh^2 \beta a} \varphi_{A_n} \\ & + \sum_{m=1}^{\infty} \frac{(-1)^m (-1)^n \cdot 2\alpha \cdot \beta^2}{b(\alpha^2 + \beta^2)^2} \frac{\psi_{b_m}}{\beta \alpha} \\ & + \sum_{m=1}^{\infty} \frac{(-1)^m \cdot 2\alpha \cdot \beta^2}{b(\alpha^2 + \beta^2)^2} \left[ 1 + \nu \left( \frac{\alpha}{\beta} \right)^2 \right] \varphi_{B_m} \\ & = \frac{(-1)^n \cdot 2}{a^3 b \beta^4} \left\{ \frac{\sinh \beta \alpha \cdot \cosh \beta \alpha - \beta \alpha}{2 \cosh^2 \beta a} \times \right. \\ & \quad \left. \left[ 1 + \frac{\cos \beta b_0}{(1-b_0/b)} \frac{(-1)^n}{\beta} \right] \right\} \quad (19) \end{aligned}$$

Similarly, substituting the equations (9) and (16) into the boundary condition Eq. (5), when  $m = 1, 2, 3, \dots$ , the equation that includes the notations  $\psi_{a_n}, \varphi_{A_n}, \psi_{b_m}, \varphi_{B_m}$  can be obtained as follows:

$$\begin{aligned}
& \sum_{n=1}^{\infty} \frac{(-1)^n (-1)^m 2\alpha^2 \beta}{a(\alpha^2 + \beta^2)^2} \frac{1}{\alpha\alpha} \psi_{an} \\
& + \sum_{n=1}^{\infty} \frac{(-1)^n 2\alpha^2 \beta}{a(\alpha^2 + \beta^2)^2} \left[ 1 + \nu \left( \frac{\beta}{\alpha} \right)^2 \right] \varphi_{,in} \\
& + \frac{\alpha b + \sinh \alpha b \cdot \cosh \alpha b}{2 \cosh^2 \alpha b} \frac{1}{\alpha\alpha} \cdot \psi_{bm} \\
& + \frac{(1-\nu)\alpha b \sinh \alpha b - 2 \cosh \alpha b}{2 \cosh^2 \alpha b} \varphi_{bm} \\
& = \frac{-(-1)^m \cdot 2}{a^4 \alpha^4} \left[ \frac{\cos \beta b_0}{(1-b_0/b)} \frac{1}{\alpha b} + \frac{\alpha b - \sinh \alpha b \cdot \cosh \alpha b}{2 \cosh^2 \alpha b} \right. \\
& \quad \left. - \frac{\cos \beta b_0}{(1-b_0/b)} \frac{\alpha b \sinh \alpha b + 2 \cosh \alpha b}{2 \alpha b \cosh^2 \alpha b} \right] \quad (20)
\end{aligned}$$

Again, substituting the equations (9) and (15) into the boundary condition equation (6), when  $n = 1, 2, 3, \dots$ , the equation that includes the notations  $\psi_{an}, \varphi_{An}, \psi_{bm}, \varphi_{Bm}$  can be obtained as follows:

$$\begin{aligned}
& - \frac{(1-\nu)\beta a \sinh \beta a - 2 \cosh \beta a}{2 \cosh^2 \beta a} \psi_{an} \\
& + \frac{(3+\nu) \sinh \beta a \cdot \cosh \beta a + (1-\nu)\beta a}{2 \cosh^2 \beta a} (1-\nu)\beta a \varphi_{,in} \\
& - \sum_{n=1}^{\infty} \frac{(-1)^n \cdot 2 \cdot \alpha^2 \beta}{b(\alpha^2 + \beta^2)^2} \left[ 1 + \nu \left( \frac{\beta}{\alpha} \right)^2 \right] \psi_{bn} \\
& - \sum_{n=1}^{\infty} \frac{2\alpha^2 \cdot \beta}{b(\alpha^2 + \beta^2)^2} (1-\nu)^2 \beta a \varphi_{bn} \\
& = \frac{(-1)^n \cdot 2}{a^2 b \beta^3} \left[ \frac{(1-\nu)\beta a \sinh \beta a}{2 \cosh^2 \beta a} + \nu - \frac{\nu}{\cosh \beta a} \right] \\
& \quad \times \left[ 1 + \frac{\cos \beta b_0}{(1-b_0/b)} \frac{(-1)^n}{\beta b} \right] \quad (21)
\end{aligned}$$

Also, substituting the equations (9) and (16) into the boundary condition equation (7), when  $m = 1, 2, 3, \dots$ , the equation that includes the notations  $\psi_{an}, \varphi_{An}, \psi_{bm}, \varphi_{Bm}$  can be obtained as follows:

$$\begin{aligned}
& - \sum_{n=1}^{\infty} \frac{(-1)^m 2\alpha \cdot \beta^2}{a(\alpha^2 + \beta^2)^2} \left[ 1 + \nu \left( \frac{\alpha}{\beta} \right)^2 \right] \psi_{an} \\
& - \sum_{n=1}^{\infty} \frac{2\alpha^2 \beta^2}{(\alpha^2 + \beta^2)^2} (1-\nu)^2 \varphi_{,in} \\
& - \frac{(1-\nu)\alpha b \sinh \alpha b - 2 \cosh \alpha b}{2 \cosh^2 \alpha b} \psi_{bm} \\
& + \frac{[(\nu+3) \sinh \alpha b \cdot \cosh \alpha b + (1-\nu)\alpha b](1-\nu)}{2 \cosh^2 \alpha b} \cdot \alpha\alpha \cdot \varphi_{bm} \\
& = \frac{(-1)^m \cdot 2}{a^3 \cdot \alpha^3} \left[ \frac{(1-\nu)\alpha b \sinh \alpha b}{2 \cosh^2 \alpha b} + \nu \cdot \frac{\cos \beta b_0}{(1-b_0/b)} - \frac{\nu}{\cosh \alpha b} \right. \\
& \quad \left. - \frac{\cos \beta b_0}{(1-b_0/b)} \frac{(1-3\nu) \sinh \alpha b \cdot \cosh \alpha b - (1-\nu)\alpha b}{2 \alpha b \cosh^2 \alpha b} \right] \quad (22)
\end{aligned}$$

By solving the above simultaneous equations, the notations

$\psi_{an}, \varphi_{An}, \psi_{bm}, \varphi_{Bm}$  can be decided. Hence, using these

notations, the deflections of the rectangular plate will be determined. In this study, the series in the above-mentioned expressions converge very rapidly, and a sufficient accuracy of the deflections is obtained by taking a few terms of  $m$  and  $n$ .

## 2.5 Bending Moment and Shearing Force in the Plate

When the deflections of the rectangular plate are determined, the magnitudes of the bending moments can be calculated. If the moments per unit length parallel to  $y$  and  $x$  axes of the rectangular plate are denoted by  $M_x$  and  $M_y$ , respectively, their expressions are shown as:

$$M_x = -D \left( \frac{\partial^2 W(x, y)}{\partial x^2} + \nu \frac{\partial^2 W(x, y)}{\partial y^2} \right) \quad (23)$$

$$M_y = -D \left( \frac{\partial^2 W(x, y)}{\partial y^2} + \nu \frac{\partial^2 W(x, y)}{\partial x^2} \right) \quad (24)$$

Similarly, the shearing forces per unit length parallel to  $y$  and  $x$  axes, and that denoted by  $Q_x$  and  $Q_y$ , respectively, their expressions are calculated by follows:

$$Q_x = -D \left( \frac{\partial^3 W(x, y)}{\partial x^3} + \frac{\partial^3 W(x, y)}{\partial x \partial y^2} \right) \quad (25)$$

$$Q_y = -D \left( \frac{\partial^3 W(x, y)}{\partial y^3} + \frac{\partial^3 W(x, y)}{\partial x^2 \partial y} \right) \quad (26)$$

Based on the analytical result of previous investigation<sup>2)</sup>, a sufficient accuracy of the bending moments of the plate can be calculated when the first five terms ( $m = n = 5$ ) of the series are taken into account. Also, the shearing forces of the plate can be calculated by taking the first ten terms ( $m = n = 10$ ) of the series. These conclusions will be used to calculate the bending moments and the shearing forces of the rectangular plates in this study.

## 3. Finite Element Method

### 3.1 Analytical Study of Finite Element Method

As a comparative investigation, the analytical results of this study and the results calculated by FEM were compared. Considering the analysis of the plates which have non-uniform sections, such as, the vertical wall of a storing-reservoir, the 3D-finite element method developed by Matsubara, et al<sup>3)</sup> was adopted. At this method, the tetrahedral element with vertex rotations was used to improve the analytical accuracy for the bending problems. The tetrahedral element with vertex rotations is shown in Fig. 2<sup>3)</sup>.

### 3.2 Bending Moments

According to the above-mentioned method of finite element analysis, only the deflections and the stresses of the bending members, such as, beams or plates can be obtained. But, the moment acting on the bending members which is needed for design can not be obtained. For this reason, the bending moments of the rectangular plate must be exchanged from the results of FEM. In this study, the signs  $\sigma_1$  and  $\sigma_2$  express the stresses at the surface of the rectangular plate, and the “plane section assumption” is applicable as mentioned earlier. The bending moment of unit width can be expressed as:

$$M = \frac{t^2}{12} (\sigma_2 - \sigma_1) \quad [N \cdot m / m] \quad (27)$$

where,  $\sigma_1$  is the compression stress with a minus sign, and  $\sigma_2$  is the tension stress with a plus sign.

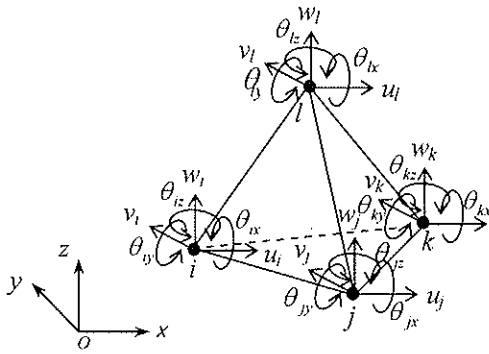


Fig. 2 Tetrahedral element with vertex rotations of FEM

## 4. Comparative Investigations of the Suggested Method and FEM

### 4.1 Rectangular Plates for Analytical Study

Considering the practical cases of this type of rectangular plates, two typical ones, which acted by the triangularly distributed regional load were analyzed for the comparative investigations. The side ratios of the rectangular plates are chosen as  $a/b=0.5$  and  $a/b=2.0$  respectively. The flexural and shear strength at fixed sides of the plate with reinforcement inside it decide the thickness of plate as shown in Figs. 3 and 4. The triangularly distributed regional loads are distributed along the length of  $2b/3$  of the rectangular plates, and was considered as the earth pressure with the angle of internal friction  $\phi=30^\circ$ . The material of the rectangular plates is concrete, it's strength, Young's modulus, Poisson's ratio are  $f_c=24\text{N/mm}^2$ ,  $E=25000\text{N/mm}^2$ ,  $\nu=1/6$ , respectively. The details and the forces of the rectangular plates are shown in Figs. 3 and 4.

### 4.2 Analytical Results of FEM

In the cases shown in Figs. 3 and 4, the elastic analysis

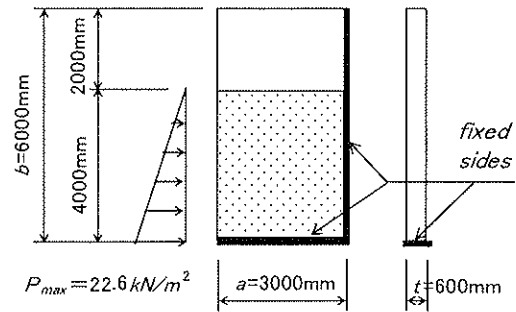


Fig. 3 Rectangular plate for the comparative study with the side ratio,  $a/b=0.5$

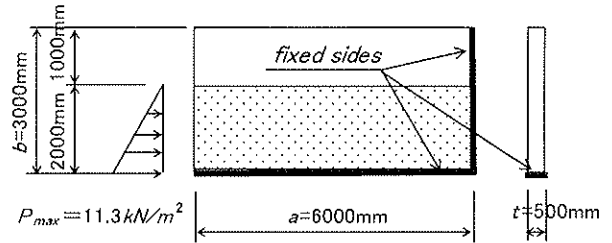


Fig. 4 Rectangular plate for the comparative study with the side ratio,  $a/b=2.0$

for the rectangular plates were carried out by FEM. Figs. 5 and 6 show the analytical results of the principal stress distributions along the plates. The maximum compression stresses  $\sigma_1$  and the maximum tension stresses  $\sigma_2$  on surface at the fixed sides of the rectangular plate are also shown in Figs. 5 and 6. The intensities of  $\sigma_1$  and  $\sigma_2$  will also be used to calculate the bending moments at the fixed sides in the next section.

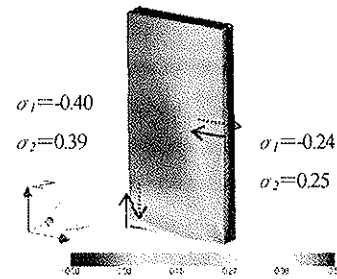


Fig. 5 Stress distributions of the rectangular plate with a side ratio of  $a/b=0.5$  (unit:  $\text{N/mm}^2$ )

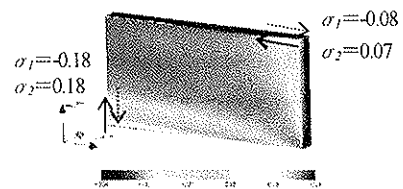


Fig. 6 Stress distributions of the rectangular plate with a side ratio of  $a/b=2.0$  (unit:  $\text{N/mm}^2$ )

### 4.3 Comparison of Bending Moments

The bending moments along the fixed sides of the rectangular plates as shown in Figs. 3 and 4 are calculated by using the suggested method. Here, the integer numbers ( $m=n=5$ ) of Fourier series were used for the calculation. Also, Eq. (27) is used to calculate the bending moments from the analytical results of the stress by FEM as shown in Figs. 5 and 6. The comparative results of the bending moments are shown in Figs. 7 and 8.

From Fig. 7, the distributions of the bending moments at side of  $x=a=3.0\text{m}$  have a good agreement between the two methods. But at side of  $y=b=6.0\text{m}$ , the maximum bending moment has the difference about 15% between the suggested method and FEM.

From Fig. 8, the distributions of the bending moments at the side  $y=b=3.0\text{m}$  have a good agreement between the two methods. But at side of  $x=a=6.0\text{m}$ , the bending moments have the maximum difference up to 10% between the suggested method and FEM.

It is shown that the maximum bending moments calculated by the suggested method are larger than that calculated by FEM. The variation of the bending moment in both the methods is not so large that it can be ignored in the design.

### 4.4 Shearing Forces

The shearing forces at fixed sides of the rectangular plates as shown in Figs. 3 and 4 are calculated by using the suggested method in this paper. Since, the shearing force is the third degree

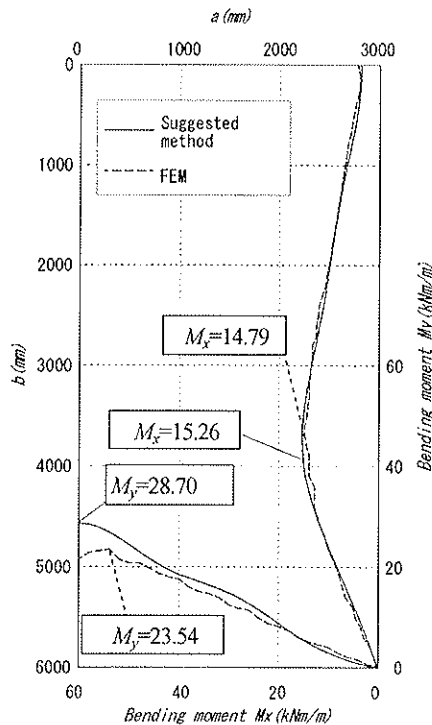


Fig. 7 Comparison of the bending moments calculated by the suggested method and FEM ( $a/b=0.5$ )

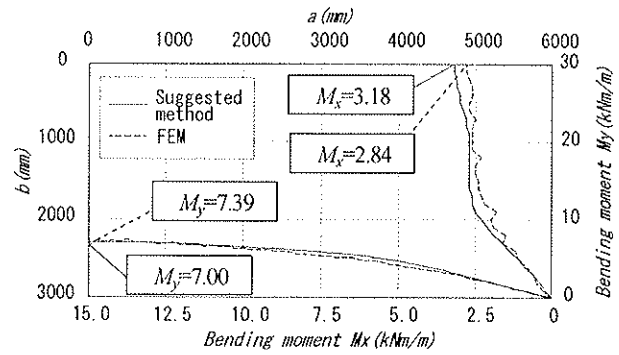


Fig. 8 Comparison of the bending moments calculated by the suggested method and FEM ( $a/b=2.0$ )

of differential of the deflection of the plates, the calculated results of shearing forces can not converge so good as the bending moments. Especially, this problem appears more obvious at the corner points.

In order to solve this problem, the second degree regression curves were used to modify the calculated results. Here, the second degree regression curves were determined by using the method of least squares from the analytical results. The abnormal values of the shearing force at the corner points were excluded. Therefore, for the sake of safety design, the maximum shearing forces of the regression curves were employed in the design. Since the shearing forces acting on the rectangular plates can not be obtained by using 3-D element as shown in Fig. 2, the comparison of the shearing force is difficult. For this reason, the results calculated by the suggested method are only shown in Figs. 9 and 10.

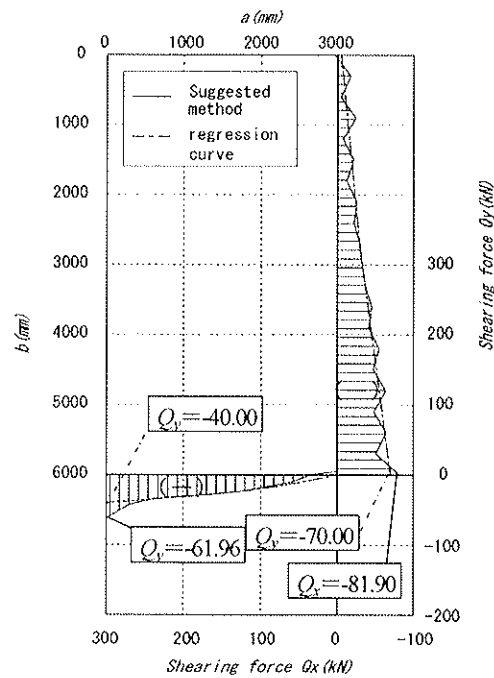


Fig. 9 The shearing forces calculated by the suggested method ( $a/b=0.5$ )

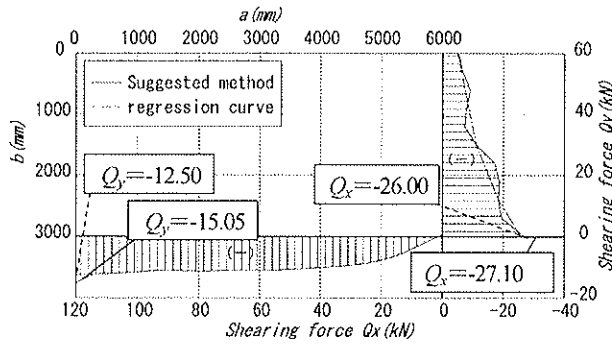


Fig. 10 The shearing forces calculated by the suggested method ( $a/b=2.0$ )

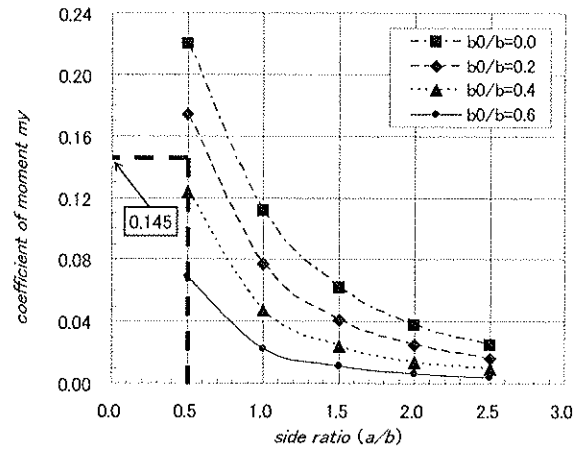


Fig. 11 Coefficient  $m_x$  of the maximum bending moments

## 5. Applications of the Analytical Results

### 5.1 Maximum Bending Moments for the Design of Rectangular Plates

The rectangular plates loaded by the triangularly distributed regional distribution forces are often used to the corner retaining walls as well as storage-reservoir. In such cases, the reinforced steel bars are arranged at the fixed side continuously, and the required quantity of the steel bars is calculated by using the maximum bending moment along the fixed sides. For this purpose, the coefficient  $m_x$  and  $m_y$  of the maximum bending moments at the fixed sides of the rectangular plates were calculated in this paper. By using  $m_x$  and  $m_y$ , the maximum bending moments acting on the fixed sides  $x=a$  and  $y=b$  can be calculated by the following expressions:

$$M_{x,\max}(a, y) = m_x \cdot a^2 \cdot P_{\max} \quad [kN \cdot m / m] \quad (29)$$

$$M_{y,\max}(x, b) = m_y \cdot a^2 \cdot P_{\max} \quad [kN \cdot m / m] \quad (30)$$

Given consideration on dimension of the rectangular plates in practical case, the side ratios of the rectangular plate was selected as  $a/b=0.5$  to  $2.5$  with a pitch of  $0.5$ , and four cases of  $b_0/b=0.0, 0.2, 0.4$  and  $0.6$  were calculated. The calculated results of the coefficient  $m_x$  and  $m_y$  are shown in Figs. 11 and 12 respectively. From Figs. 11 and 12, there is a tendency that the coefficients  $m_x$  and  $m_y$  decrease with the increase of the side ratios  $a/b$ .

### 5.2 Maximum Shearing Forces for the Design of Rectangular Plates

For the same purpose as explained in section 5.1, the coefficients  $q_x$  and  $q_y$  of the maximum shearing forces at the fixed sides of the rectangular plates were calculated, and the maximum shearing forces acting on the fixed sides  $x=a$  and  $y=b$  can be calculated by the following expressions:

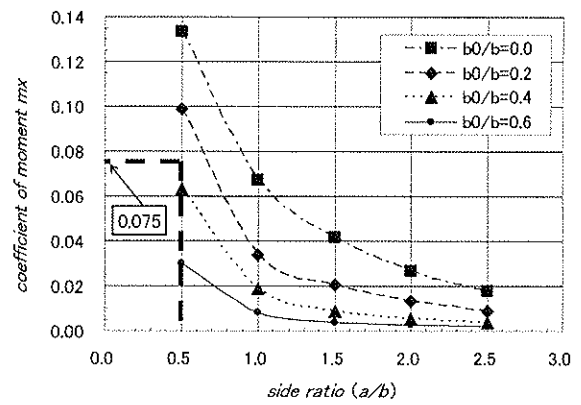


Fig. 12 Coefficient  $m_y$  of the maximum bending moments

$$Q_{x,\max}(a, y) = q_x \cdot a \cdot P_{\max} \quad [kN] \quad (31)$$

$$Q_{y,\max}(x, b) = q_y \cdot a \cdot P_{\max} \quad [kN] \quad (32)$$

The same manner as shown in section 5.1 was used to calculate the coefficients  $q_x$  and  $q_y$ . Figs. 13 and 14 show the calculated results.

From Figs. 13 and 14, the coefficients  $q_x$  and  $q_y$  have the same tendency that the coefficients  $q_x$  and  $q_y$  decrease with the increase of side ratios  $a/b$ . Because of the rectangular plates acting by the triangularly distributed regional loads, the values of  $q_x$  are very near to each other at the same side ratio.

For example, in case of Fig. 7, side ratio  $a/b=0.5$ ,  $a=3.0m$ ,  $b_0/b=1/3$ , and  $P_{\max}=22.6 \text{ kN/m}^2$ , by using Figs. 11 to 14, the coefficients  $m_x = 0.075$ ,  $m_y = 0.145$ ,  $q_x = 1.04$ , and  $q_y = 0.64$  are obtained. On substituting these coefficients to Eqs. (29), (30), (31) and (32), the maximum moments  $M_{y,\max}(a, y)=15.3 \text{ kN-m/m}$ ,  $M_{x,\max}(x, b)=29.5 \text{ kN-m/m}$ , and the maximum shearing forces  $Q_{x,\max}(a, y)=70.5 \text{ kN}$ ,  $Q_{y,\max}(x, b)=43.4 \text{ kN}$  are calculated respectively.

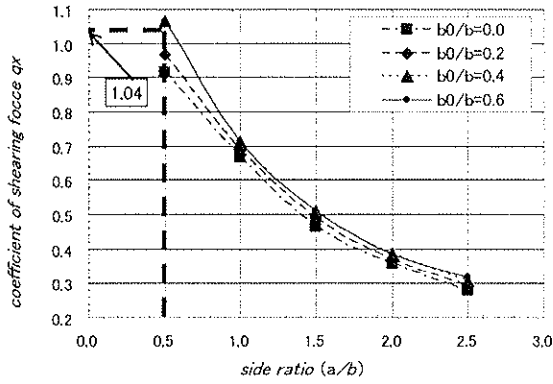


Fig.13 Coefficient  $q_x$  of the maximum shearing force

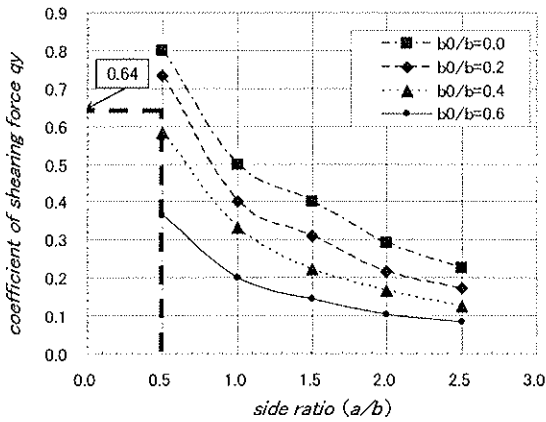


Fig.14 Coefficient  $q_y$  of the maximum shearing force

## 6. Conclusions

This paper shows the analytical study and application of rectangular plates with two adjacent sides fixed and other two sides free under triangularly distributed regional loads. The followings are concluded from this study:

- (1) Based on the Fourier series analytical method<sup>1)</sup>, the analytical results for the rectangular plates with two adjacent sides fixed and two sides free under triangularly distributed regional loads are presented. Hence, the figures of the coefficients  $m_x$  and  $m_y$  of the maximum bending moments and the coefficients  $q_x$  and  $q_y$  of the maximum shearing forces on the fixed sides of the rectangular plates were presented for the designer.

- (2) A comparative investigation between the suggested method and FEM was carried out. The results show that the distributions of the bending moments are in good agreement between the two methods. Some difference between the suggested method and FEM is caused by using Eq.(27) of FEM. But, the variation of the bending moment in both the methods is not so large that it can be ignored in the design.
- (3) The maximum bending moments calculated by the suggested method are larger than that calculated by FEM. For this reason, the safety design can be ensured when this method is used.
- (4) In the case of the shearing forces, the second degree regression curves were used to modify the calculated results. Here, the second degree regression curves were determined by using the method of least squares and the abnormal values of the shearing force at the corner points were excluded. Therefore, for the sake of safety design, the maximum shearing forces of the regression curves were employed in the design.

## ACKNOWLEDGEMENTS

The authors are grateful to Prof. Tetsuo YAMAKAWA and Prof. Kyosi KOMORI for their valuable advice toward this study.

## REFERENCES

- 1) Higashi, Y. and Komori, K: Series-11 of architectural structure, Slab structure, 1966
- 2) Kaneda, K. Takamine, T. Chinen, Y. and Iraha, S.: An analytical study and application of earth pressures loaded rectangular plates in the condition of two adjacent sides fixed and the other sides free, Journal of structural engineering, Vol.50A, 1025-1034, 2004.3
- 3) Matsubara, H. Iraha, S. Tomiyama, J. Yamashiro, T. and Yagawa, G: Free mesh method using tetrahedral element including the vertex rotations, JSCE, No.766/I-68, 97-107, 2004.7

(Received: April 15 2005)